Molecular Therapy
Nucleic Acids
Original Article

miR-214 Attenuates Aortic Valve Calcification by Regulating Osteogenic Differentiation of Valvular Interstitial Cells

Ning Li,[1,3,4] Yifan Bai,[1,4] Guangwei Zhou,[1,4] Ye Ma,[1] Mengwei Tan,[1] Fan Qiao,[1] Xin Li,[1] Ming Shen,[2] Xiaowei Song,[2] Xianxian Zhao,[2] Xiaohong Liu,[1] and Zhiyun Xu[1]

[1]Department of Cardiothoracic Surgery, Changhai Hospital, Second Military Medical University, Shanghai, 200433, China; [2]Department of Cardiology, Changhai Hospital, Second Military Medical University, Shanghai, 200433, China; [3]Department of Cardiothoracic Surgery, Naval Medical Center of PLA, Second Military Medical University, Shanghai, 200052, China

Calcific aortic valve disease (CAVD) is a common heart valve disease in aging populations, and aberrant osteogenic differentiation of valvular interstitial cells (VICs) plays a critical role in the pathogenesis of ectopic ossification of the aortic valve. miR-214 has been validated to be involved in the osteogenesis process. Here, we aim to investigate the role and mechanism of miR-214 in CAVD progression. miR-214 expression was significantly downregulated in CAVD aortic valve leaflets, accompanied by upregulation of osteogenic markers. Overexpression of miR-214 suppressed osteogenic differentiation of VICs, while silencing the expression of miR-214 promoted this function. miR-214 directly targeted ATF4 and Sp7 to modulate osteoblastic differentiation of VICs, which was proved by dual luciferase reporter assay and rescue experiment. miR-214 knockout rats exhibited higher mean transvalvular velocity and gradient. The expression of osteogenic markers in aortic valve leaflets of miR-214 knockout rats was upregulated compared to that of the wild-type group. Taken together, our study showed that miR-214 inhibited aortic valve calcification via regulating osteogenic differentiation of VICs by directly targeting ATF4 and Sp7, indicating that miR-214 may act as a profound candidate of targeting therapy for CAVD.

INTRODUCTION

Calcific aortic valve disease (CAVD) is a common heart valve disease in aging populations, with fibrosis and calcification as its pathological characteristics. At present, there is no conservative treatment scheme available for CAVD patients, and aortic valve replacement is the only choice when these patients are accompanied with obvious clinical symptoms and hemodynamic disorder.[1] It is reported that CAVD is a pathological process involving multiple factors that can be divided into 2 phases: the initiation phase and the advanced phase.[2,3] Aortic valve leaflets can gradually progress to valvular sclerosis during the initiation phase without any symptoms, and the pathological mechanism is similar to that of atherosclerosis, including valve endothelial damage, lipid deposition, and inflammatory reaction. The advanced stage is characterized by extracellular fibrosis and calcification. The aberrant differentiation of valvular interstitial cells (VICs) to osteoblasts may act as the theoretical basis of ectopic ossification of the aortic valve.[4]

ATF4 has been confirmed to be a pivotal regulatory factor in the classical signaling pathway of endoplasmic reticulum stress (ERS), which may determine the fate of cells under various adverse conditions like amino acid deprivation. Meanwhile, it is also indispensable during development and differentiation of eyes, bones, and the hematopoietic system.[5–7] It is worth mentioning that ATF4 is involved in the regulation of osteoblasts at a more mature stage. Zhang et al.[8] have verified that ATF4 knockout (KO) mice exhibited an osteopenic phenotype, accompanied by reduced expression of osteocalcin (OCN) and type I collagen. However, the understanding of ATF4 in valvular heart disease was limited.

MicroRNA is a type of non-coding RNA with a length of about 18–26 bp. Its post-transcriptional regulatory ability is mainly achieved by promoting the degradation of its target mRNA or silencing it. miR-214, which is encoded by the DNM3 gene, is quite conserved in vertebrates and can maintain the homeostasis of bone tissue by regulating the activity of osteoblasts and osteoclasts.[9–13] DNM3 knockout mice exhibited skeletal abnormalities after birth, including craniofacial hypoplasia, dorsal neural arch and vertebral spinous process defects, and bone loss, suggesting that the DNM3 gene is important for skeletal development.[14] In addition, Roberto et al.[15] have demonstrated that overexpression of miR-214 *in vivo* hindered the formation of cranial cartilage in zebrafish. In contrast, Yang et al.[16] found that inhibition of miR-214 in rat bone marrow

Received 15 April 2020; accepted 10 October 2020;
https://doi.org/10.1016/j.omtn.2020.10.016.

[4]These authors contributed equally to this work

Correspondence: Xiaohong Liu, Department of Cardiothoracic Surgery, Changhai Hospital, Second Military Medical University, Shanghai, 200433, China.
E-mail: 2206100117@csu.edu.cn
Correspondence: Zhiyun Xu, Department of Cardiothoracic Surgery, Changhai Hospital, Second Military Medical University, Shanghai, 200433, China.
E-mail: xuzhiyunsh@163.com

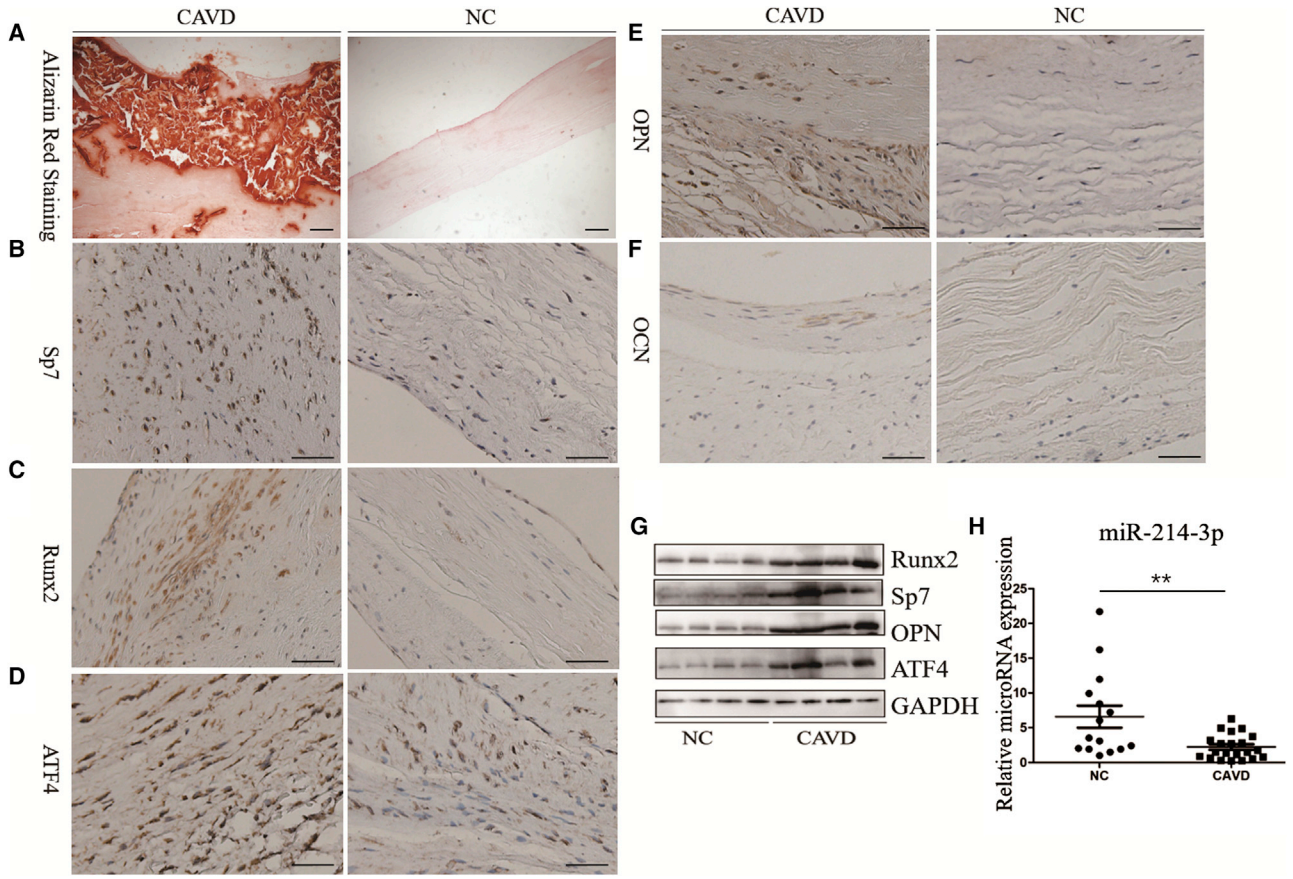

Figure 1. Histological and Molecular Analysis of CAVD Valve Leaflets

(A) Representative alizarin red staining of aortic valve of CAVD and NC patients. Aortic valve samples in NC group were obtained from 15 recipients who suffered dilated cardiomyopathy and received heart transplantation in our cardiac center. Calcium deposition (red) can be observed at fibrous layer of aortic valve in CAVD patients. Scale bar, 200 μm. (B–F) Representative immunohistochemical staining of osteogenic proteins (B) Sp7, (C) Runx2, (D), ATF4, (E) OPN, and (F) OCN of aortic valve. The expression of osteogenic proteins was upregulated in CAVD aortic valve. Scale bars, 50 μm. (G) Western blotting analysis of osteogenic proteins of the aortic valve. The expression of osteogenic proteins was upregulated in CAVD aortic valve. (H) Quantitative real-time PCR analysis of miR-214 of aortic valve. The expression of miR-214 was significantly downregulated in CAVD aortic valve; n = 15 for NC group and n = 21 for CAVD group. CAVD, calcific aortic valve disease; NC, negative control; ATF4, Activating Transcription Factor 4; OPN, Osteopontin; OCN, Osteocalcin. **$p < 0.01$.

mesenchymal stem cells by lentiviral vectors could promote its osteogenic differentiation. Extracellular vesicles containing miR-214 can be transferred from osteoclasts into osteoblasts and then inhibit osteoblast function.[17,18] Taken together, these results suggest that miR-214 may be indispensable for osteogenic differentiation.

Considering CAVD is an ectopic osteogenesis process, we hypothesize that miR-214 is involved in the pathological regulation of aortic stenosis. miR-214 has been identified to be a side- and shear-dependent microRNA that regulated mechanosensitive genes in the aortic valve.[19] Salim et al.[20] found that overexpression of miR-214 inhibited aortic valve calcification when aortic valve leaflets were cultured in osteogenic medium combined with cyclic stretch. As far as we know, the expression profile of miR-214 in the aortic valve was found to be different in different research groups, and the function and underlying mechanism of miR-214 in CAVD remain unclear.[21–24]

In this work, we aimed to investigate the function and mechanism of miR-214 in osteogenic differentiation of VICs *in vitro*, as well as the role of miR-214 in aortic valve calcification in a CAVD rat model *in vivo*.

RESULTS

miR-214 Was Downregulated in CAVD Aortic Valve Leaflets

Previous studies have verified that the aortic valve leaflet can be divided into fibrosa, spongiosa, and ventricular layers from the aortic side to the ventricular side. VICs are distributed in all three layers and a monolayer of valve endothelial cells (VECs) covering both sides.[2,3] To verify the accuracy of the collected aortic valve samples, we performed alizarin red staining to identify the calcium deposition. As shown in Figure 1A, the calcification nodules were frequently located at the fibrous layer of valve leaflets in CAVD group. Meanwhile, the expression of osteogenic markers, including Runx2, Sp7, ATF4, and

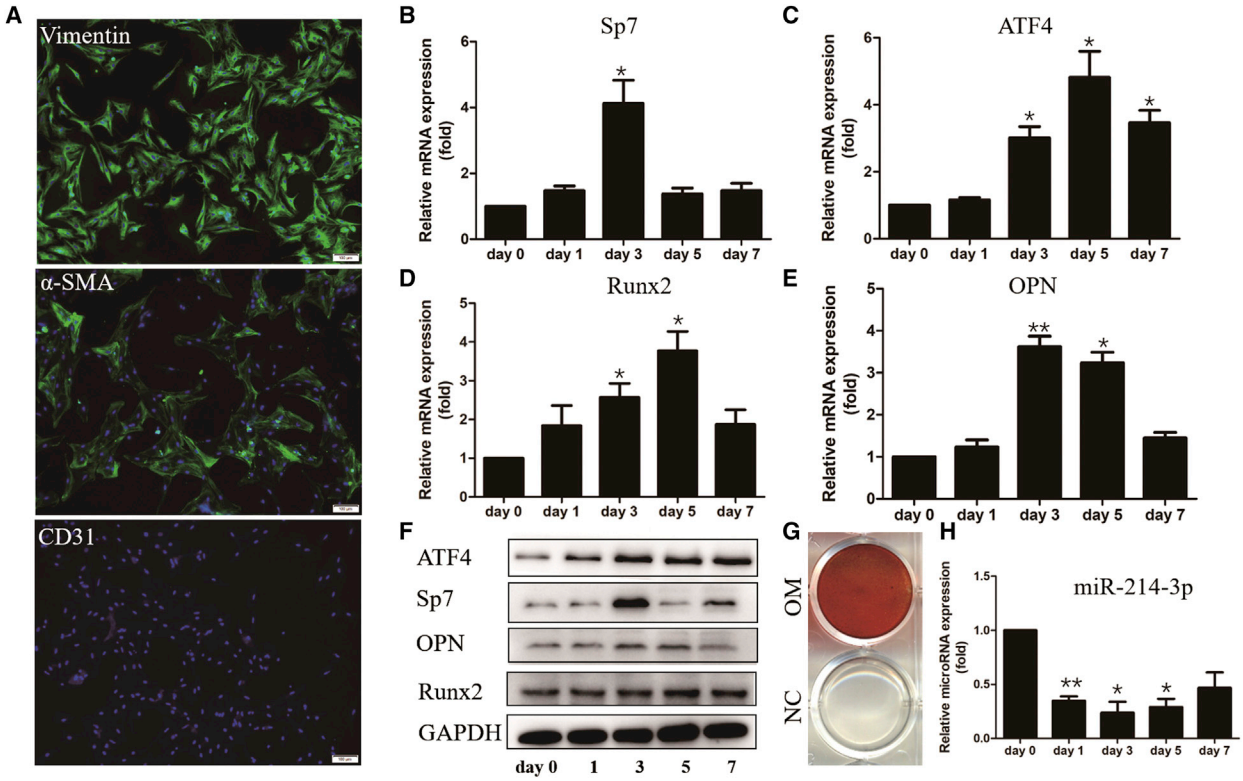

Figure 2. VICs Isolation and Osteogenic Induction *In Vitro*

(A) Representative immunofluorescence staining of vimentin (green), α-SMA (green), and CD31 of VICs. The positive staining of vimentin and negative staining of CD31 indicated the harvested cells were VICs. The nuclei were counterstained with 4',6-diamidino-2-phenylindole (DAPI) (blue). Scale bar, 100 μm. (B–E) Quantitative real-time PCR analysis of osteogenic markers of VICs after osteogenic induction *in vitro*: (B) Sp7; (C) ATF4; (D) Runx2; and (E) OPN. The expression of osteogenic genes was significantly upregulated at day 3. (F) Western blotting analysis of osteogenic proteins of VICs after osteogenic induction *in vitro*. The expression of osteogenic proteins was upregulated at day 3. (G) Representative alizarin red staining (red) of VICs after osteogenic induction for 7 days *in vitro*. (H) Quantitative real-time PCR analysis of miR-214 of VICs after osteogenic induction *in vitro*. The expression of miR-214 was significantly downregulated at day 1 and maintained at a lower level until day 7. VICs, valvular interstitial cells; OM, osteogenic induction medium. *$p < 0.05$, **$p < 0.01$.

OPN, was upregulated in CAVD samples, which was verified by immunohistochemical staining and western blotting (Figures 1B–1G), indicating the existence of osteogenic differentiation in VICs. However, the negative staining of OCN in aortic valve leaflets may suggest that aortic valve calcification was a pathological process of immature osteogenesis (Figure 1F). Lastly, the expression of miR-214-3p was significantly downregulated in CAVD valve samples compared to that of negative control group (Figure 1H). These results suggest that miR-214-3p plays an important role in the pathological process of VICs from CAVD patients.

VICs Isolation and Osteogenic Induction *In Vitro*

To determine the function of miR-214 in osteogenic differentiation of VICs, we isolated VICs from aortic valves by enzymatic digestion, and then the harvested VICs were used to construct an osteogenic induction model *in vitro*. The isolated VICs were identified by immunofluorescence. As shown in Figure 2A, the positive staining of vimentin and negative staining of CD31 demonstrated the harvested cells were pure VICs without a mixture of VECs. Additionally, the positive staining rate of α-SMA was about 60%, which may indicate the activation of VICs. The expression of osteogenic markers, including Runx2, Sp7, ATF4, and OPN, was significantly upregulated at day 3 after osteogenic induction, which was verified by quantitative real-time PCR and western blotting (Figures 2B–2F). We further evaluated the effect of osteogenic induction by alizarin red staining at day 7 after osteogenic induction (Figure 2G). Lastly, we detected the expression of miR-214 in VICs after osteogenic induction and found that miR-214 was significantly suppressed before the upregulation of osteogenic markers (Figure 2H). These results prompted the assumption that the downregulation of miR-214 may play a vital role in osteogenic differentiation of VICs.

miR-214 Inhibits Osteoblastic Differentiation of VICs

To validate the inhibitory effect of miR-214 in osteoblastic differentiation of VICs, we overexpressed and knocked down miR-214 in VICs by transfected agomiR-214 and antagomiR-214, respectively. The effect of overexpression of miR-214 in VICs was verified by quantitative real-time PCR, western blotting, and alizarin red staining. As shown

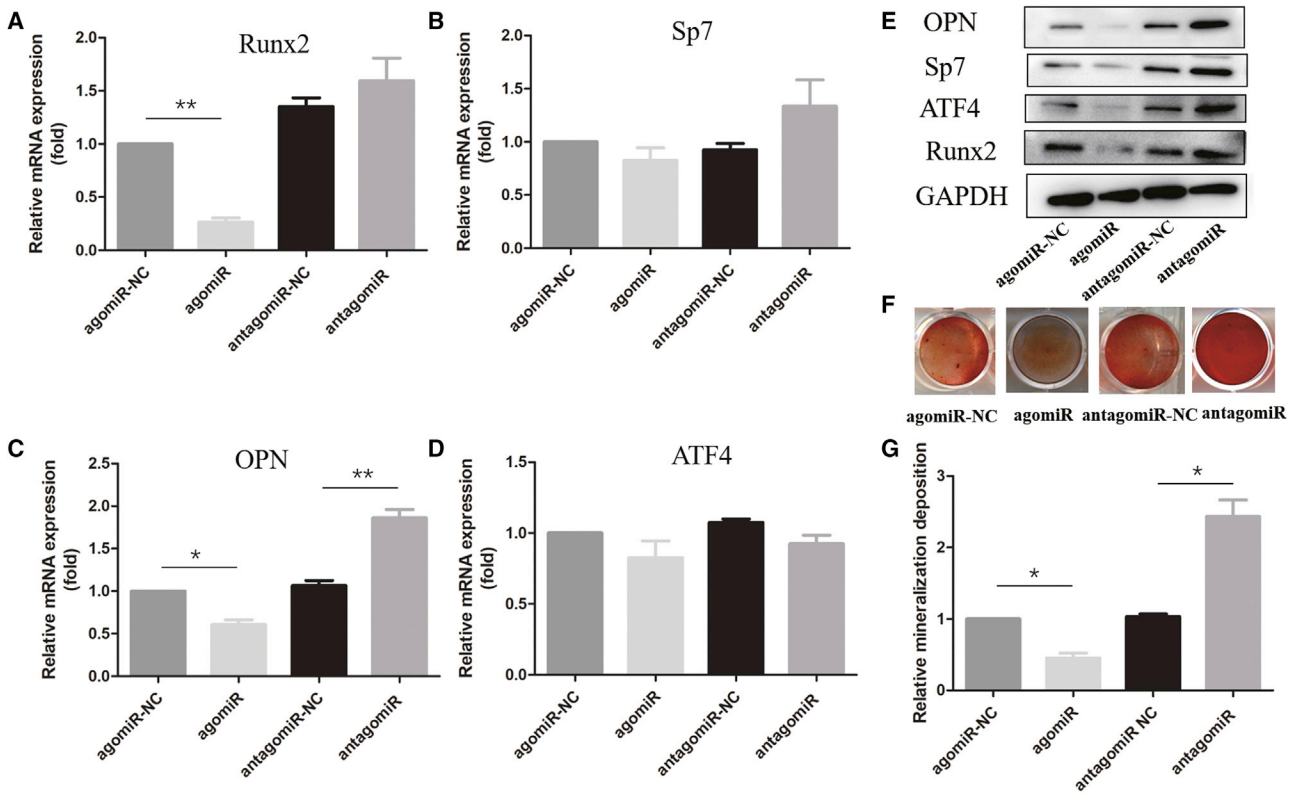

Figure 3. miR-214 Inhibits Osteoblastic Differentiation of VICs

(A–D) Quantitative real-time PCR analysis of osteogenic genes (A) Runx2, (B) Sp7, (C) OPN, and (D) ATF4 of VICs after overexpression and knockdown of miR-214. The mRNA expression of Runx2 and OPN were significantly downregulated after transfection of agomiR-214. (E) The protein expression of Runx2, OPN, ATF4, and Sp7 were markedly suppressed after transfection of agomiR-214. (F) Alizarin red staining of calcium deposition. (G) Relative mineralization deposition was measured by spectrophotometry when alizarin red stain was released from the cell matrix by incubation with 10% acetic acid solution. Calcium deposition was significantly reduced after transfection of agomiR-214 and was promoted by antagomiR-214. *$p < 0.05$, **$p < 0.01$.

in Figures 3A–3D, the mRNA expression of Runx2 and OPN was suppressed after transfection of agomiR-214. Conversely, the mRNA expression of OPN was promoted by silencing miR-214. In addition, the mRNA expression of Sp7 and ATF4 was not significantly altered under different expression levels of miR-214 by transfection of agomiR-214 or antagomiR-214.

The protein expression of OPN, Sp7, ATF4, and Runx2 was inhibited after overexpression of miR-214 (Figure 3E). Meanwhile, calcium deposition was significantly attenuated by transfection of agomiR-214 but accelerated by antagomiR-214 (Figures 3F and 3G). Taken together, miR-214 inhibited osteoblastic differentiation of VICs *in vitro*.

miR-214 Directly Targets ATF4 and Sp7

We further explored the underlying molecular mechanism of miR-214 in regulation of osteogenic differentiation. Among the putative targets, ATF4 and Sp7 were crucial for the ossification process. Considering the similarity of the pathological characteristics between CAVD and osteogenesis, we focused on ATF4 and Sp7 for further study (Figure 4A). Luciferase reporter plasmids containing the 3′-UTR of ATF4, Sp7, or corresponding mutant sequences were constructed. Overexpression of miR-214 significantly inhibited the luciferase activity of wild-type (WT)-ATF4-3′-UTR and WT-Sp7-3′-UTR (Figures 4B and 4C). Conversely, the vector containing the mutant sequence abolished this inhibition, suggesting that miR-214 could directly target ATF4 and Sp7 with specificity.

To investigate whether ATF4 and Sp7 were vital for the inhibitory effect of miR-214 in osteogenic differentiation of VICs, we performed a rescue experiment. We identified that the protein expression of ATF4 in VICs was inhibited after transfection with si-ATF4. As a result, the mineralization deposition was significantly attenuated by transfection of si-ATF4, in contrast to the aggravation effect induced by antagomiR-214. Of note, the aggravation effect of mineralization deposition induced by antagomiR-214 was also abolished by co-transfection with si-ATF4 (Figure 4D). Taken together, we confirmed that ATF4 was a functional target of miR-214 in the osteogenic differentiation of VICs. An identical result related to Sp7 was seen after analyzing the results

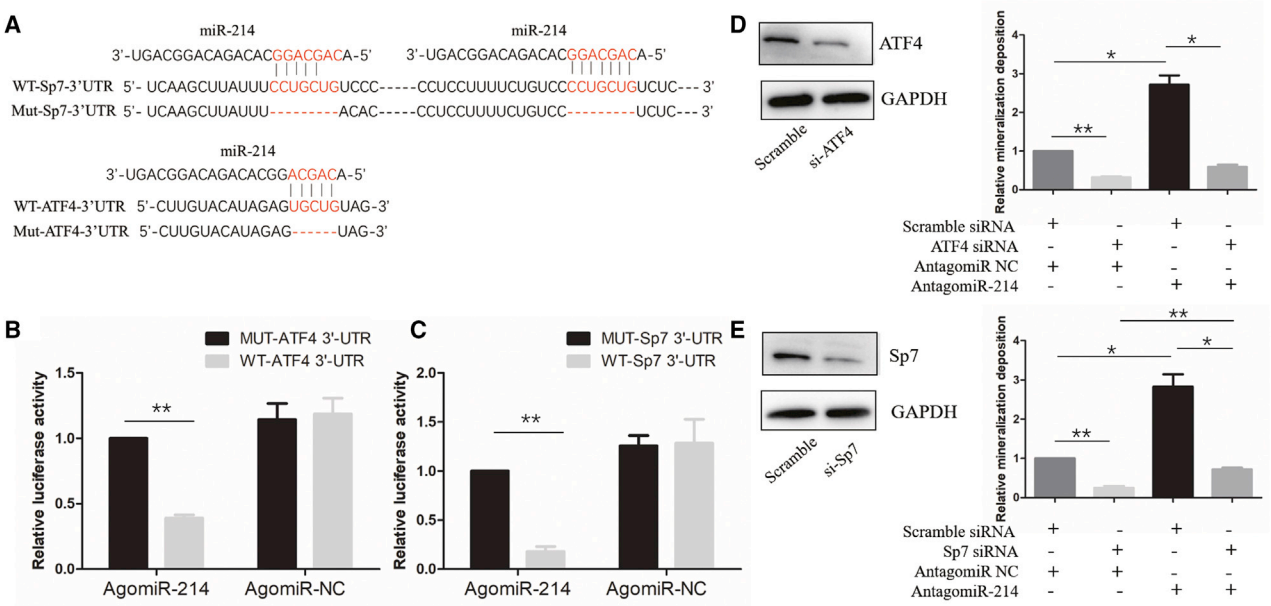

Figure 4. miR-214 Directly Targets ATF4 and Sp7

(A) Bioinformatic analysis of putative binding site (highlighted in red) of miR-214. The mutant sequence is shown below. (B and C) The luciferase activity of WT-ATF4-3′-UTR (B) and WT-Sp7-3′-UTR (C) was significantly inhibited by agomiR-214. Mutant vector was set as control. (D) The expression of ATF4 was downregulated after transfection with si-ATF4. Silencing the expression of ATF4 significantly reduced the calcium deposition of VICs. The calcium deposition induced by antagomiR-214 was alleviated by si-ATF4. (E) The expression of Sp7 was downregulated after transfection with si-Sp7. Silencing the expression of Sp7 significantly reduced the calcium deposition of VICs. The calcium deposition induced by antagomiR-214 was abolished by si-Sp7. WT, wild-type. *$p < 0.05$, **$p < 0.01$.

in Figure 4E. The mineralization deposition was significantly inhibited by transfection of si-Sp7; moreover, the aggravation effect of mineralization deposition induced by antagomiR-214 was also abolished by co-transfection with si-Sp7.

miR-214 Knockout Promotes Aortic Valve Calcification *In Vivo*

A combination of Western diet for 4 months and intraperitoneal injection of vitamin D for 1 month was applied to generate aortic valve calcification of miR-214 knockout rats, as evidenced by positive result of Alizarin red staining at aortic valve and aortic wall (Figures S1–S3). The hemodynamic parameters of the aortic valve were assessed by echocardiography. As shown in Figure 5A, knockout of miR-214 led to increment of transvalvular velocity in contrast to WT rats. Alizarin red staining was used to detect the mineralized nodule formation of the aortic valve. Monocyte infiltration and calcium deposition were observed in knockout rats (Figures 5B and 5C). In addition, no significant difference of the left ventricular ejection fraction and aortic valve area were observed between WT, knockout, and heterozygous groups (Figures 5D and 5E). miR-214 knockout rats exhibited significantly higher mean transvalvular velocity and gradient compared to WT rats. Lastly, we detected the expression of Runx2, Sp7, OPN, and ATF4 in the aortic valve of rats. As expected, miR-214 knockout rats exhibited higher expression of Runx2, Sp7, OPN, and ATF4 by immunohistochemical staining compared to the WT group (Figure 6). In summary, miR-214 knockout promoted aortic valve calcification *in vivo*.

DISCUSSION

The role of miR-214 in vertebrate skeletal development, which was achieved by modulating the activity of osteoblasts and osteoclasts, has been widely documented.[9,10] However, its function in the cardiovascular system is poorly understood. Several studies have highlighted the importance of miR-214 in valvular calcification,[25] but the study related to the function and mechanism of miR-214 in CAVD is still in its infancy. Song et al.[22] reported in their earlier study that the expression of miR-214 in CAVD valve samples was decreased by microRNA array analysis. In this work, we first identified the downregulation of miR-214 in CAVD aortic valve leaflets by quantitative real-time PCR, and we also found that knockout of miR-214 promoted aortic valve calcification *in vivo*, indicating that miR-214 plays a crucial role in regulating the ectopic osteogenesis process of CAVD.

Another outstanding finding of this study is that miR-214 inhibits osteogenic differentiation of VICs by targeting ATF4 and Sp7. Previous studies have confirmed that osteogenic differentiation of VICs was involved in the pathological process of ectopic calcification of aortic valve leaflets. However, the underlying mechanism has not been elucidated. ATF4 was previously regarded as a marker of ERS, and the PERK-ATF4 pathway, which is a typical signaling of ERS, may contribute to vascular calcification.[26] Recently, ATF4 has been reported to be upregulated in calcified aortic tissues.[27,28] In this paper, we found that downregulation of ATF4 expression inhibited mineralization of VICs, indicating the functional importance of ATF4 in aortic valve

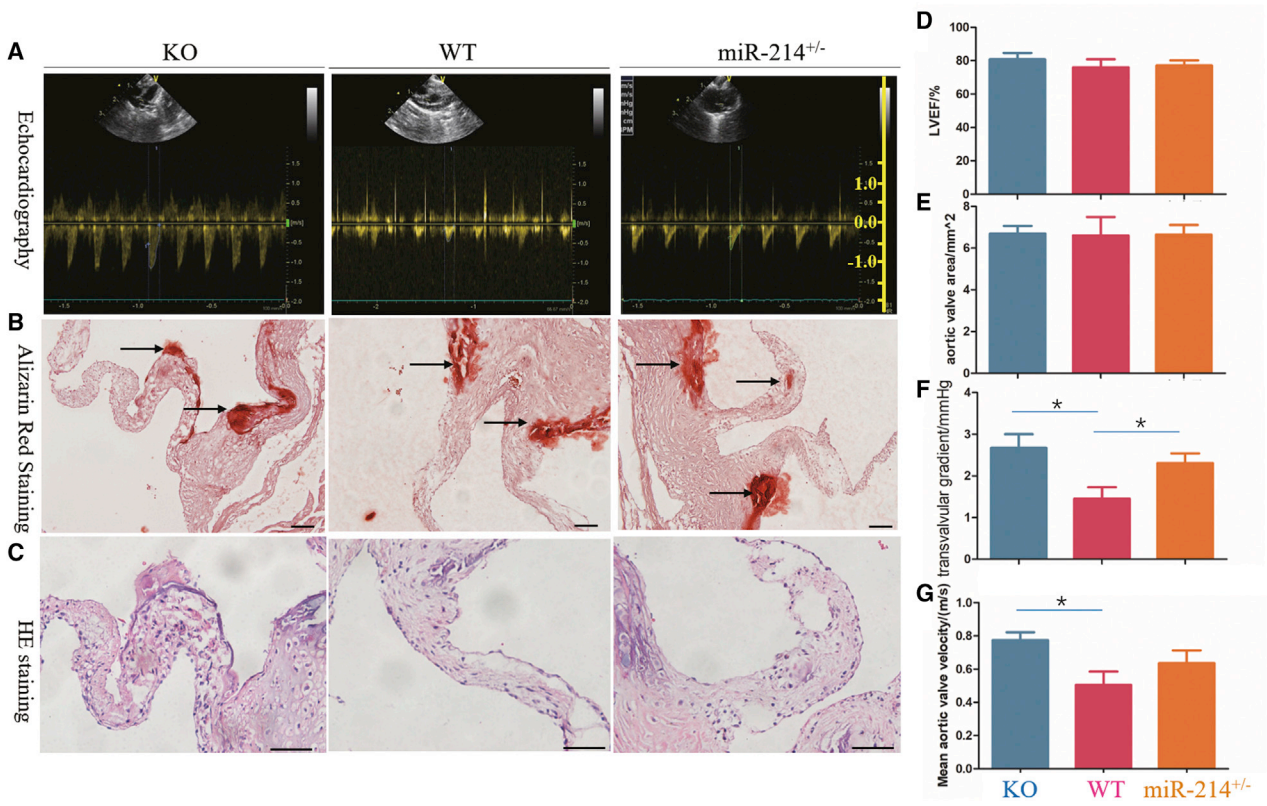

Figure 5. miR-214 KO Promotes Aortic Valve Calcification *In Vivo*

(A) Echocardiography analysis of CAVD rats. (B) Alizarin red staining of calcium deposition. Calcification nodules (black arrow) could be observed at the fiber layer of aortic valve and aortic wall in KO and heterozygous groups. (C) H&E staining of aortic valve. Monocyte infiltration could be observed at the aortic root in KO and heterozygous groups. (D and E) LVEF (D) and aortic valve (E) area of CAVD rats. There were no significant differences in LVEF and aortic valve area among 3 groups. (F and G) Transvalvular gradient (F) and mean aortic valve velocity (G) of aortic valve. miR-214 KO led to increased mean transvalvular velocity and gradient compared to WT group. KO, knockout; LVEF, left ventricular ejection fraction; H&E, hematoxylin and eosin. Scale bars, 50 μm. *$p < 0.05$.

calcification. The mechanism of ATF4 in regulating osteogenesis may be as follows: (1) ATF4 can directly regulate the expression of its downstream proteins, including OCN and RANKL. OCN is an important extracellular matrix secreted by osteoblasts in bone tissue, and RANKL could regulate osteoclast function.[29,30] (2) ATF4 could promote efficient input of amino acids and thus promote protein synthesis of osteoblasts. (3) ATF4 is necessary for type I collagen synthesis, although ATF4 is not directly involved in the transcriptional regulation of type I collagen.[31] In addition, we noticed that knockdown of ATF4 or Sp7 did not block the calcification progression of VICs totally, suggesting that there are other regulators involved in the process of CAVD.

It is worth mentioning that miR-214 may serve as a potential target for small-molecule drug delivery systems.[32] Wang et al.[33] have demonstrated that the function of osteoblast activity promotion was achieved by knockdown of miR-214 by adenoviral vectors in an osteonecrosis rat model. A parallel result was obtained by sponging miR-214 through baculovirus vector, and a combination of Bone Morphogenetic Protein 2 could promote the healing effect of bone synergistically.[34] The dual-regulatory function, including inhibiting osteoblast activity and enhancing osteoclast activity, of miR-214 may play an important role in regulating osteogenesis activities.[10,12,33] In addition, targeted materials loading with miR-214 may also have profound prospects. Sun et al.[35] have designed polyurethane nanomicelles modified by osteoblast-targeting peptides as delivery systems to deliver antagomiR-214 to osteoblasts, which was proved to be successful in an ovariectomized osteoporosis mouse model, since bone mass and formation were improved significantly. These results suggest that miR-214 may provide an alternative avenue for targeted treatment of CAVD, but this needs further exploration.

In conclusion, miR-214 inhibits aortic valve calcification by inhibiting the expression of two vital osteogenic transcription factors, namely ATF4 and Sp7, suggesting the potential therapeutic application of miR-214 for CAVD.

MATERIALS AND METHODS

Human Aortic Valve Sample Collection

This study was approved by the ethics committee of Changhai Hospital, Second Military Medical University. The calcific aortic valve

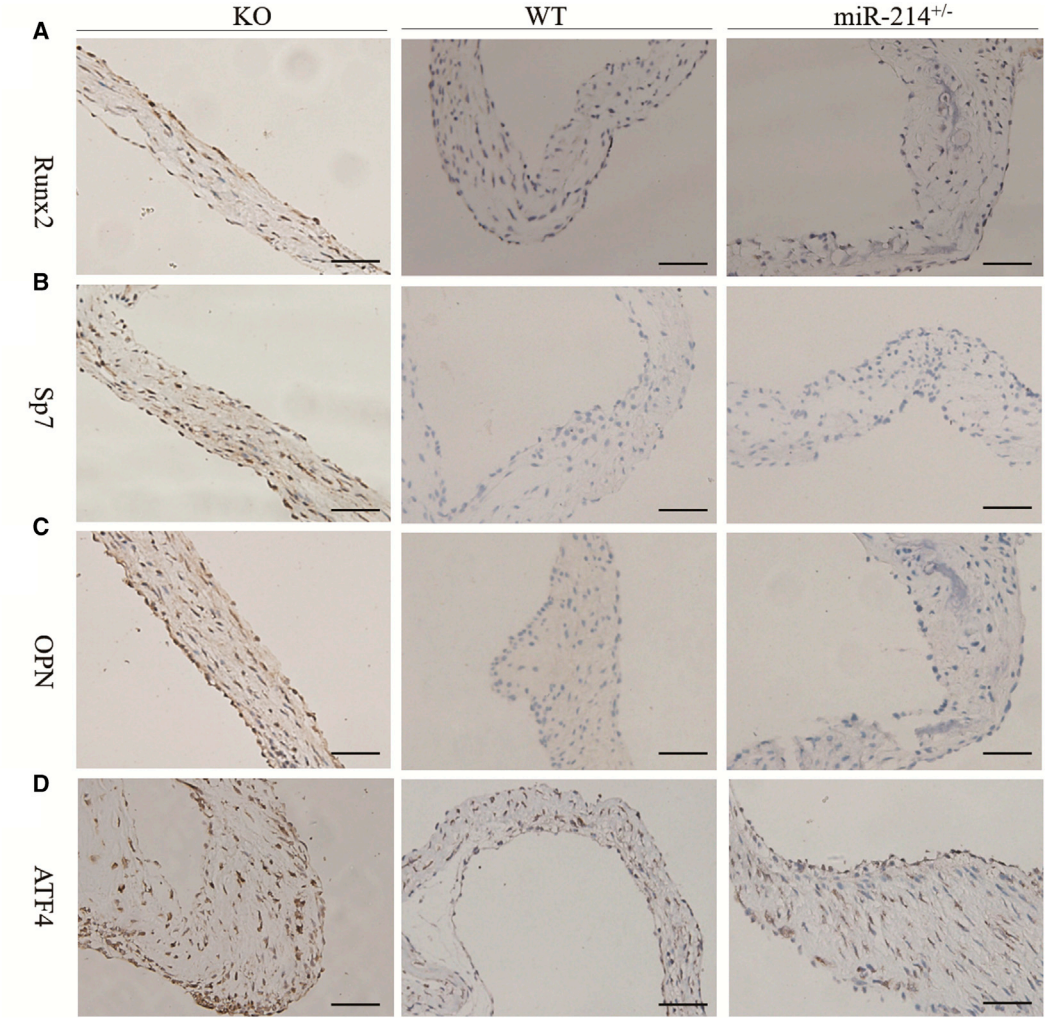

Figure 6. miR-214 KO Promotes Osteoblastic Differentiation of VICs *In Vivo*

(A–D) Representative immunohistochemical staining of osteogenic proteins of aortic valve of CAVD rats: (A) Runx2; (B) Sp7; (C) OPN; and (D) ATF4. The expression of osteogenic proteins was upregulated in the miR-214 KO group compared to that of the WT group. Scale bars, 50 μm.

samples were collected from 21 CAVD patients who underwent aortic valve replacement in our institution under informed consent. Exclusion criteria were patients diagnosed with non-stenotic or congenital aortic valve disease, infectious endocarditis, and rheumatic aortic valve disease. The control aortic valve samples were obtained from 15 recipients who suffered dilated cardiomyopathy and received heart transplantation in our center. All samples were resected intraoperatively and stored in liquid nitrogen immediately. Alizarin red staining was performed to confirm the accuracy of these obtained specimens. The demographic data of the CAVD group and the control group are listed in Table 1.

VIC Isolation and Cell Culture

The aortic valve leaflets were harvested from the aforementioned patients in the control group and immersed in pre-cooling phosphate buffered solution (PBS). The VECs were scraped away after digestion of type II collagenase for 15 min at 37°C. Then, the valves were rinsed by PBS for 3 min thrice; the tissues were then cut into pieces and digested for an additional 2 h at 37°C in a shaker. Primary VICs were obtained and seeded in DMEM supplemented with 100 U/mL penicillin, 100 μg/mL streptomycin, and 10% fetal bovine serum at 37°C under a humidified 5% CO_2 incubator. All experiments were performed using isolated VICs from passages 2 and 5.

Osteogenic Differentiation of VICs

Osteogenic differentiation was induced by culturing VICs with osteogenic differentiation medium (complete medium supplemented with 50 μg/mL ascorbic acid, 2 mmol/L sodium dihydrogen phosphate dihydrate, and 10^{-7} mol/L insulin). The osteogenic differentiation medium was changed every 2–3 days.

Table 1. Patient Profiles

Variables	CAVD (n = 21)	Control (n = 15)	p Value
Age, years	57.2 ± 7.8	48.7 ± 14.7	0.053
Male, n (%)	15 (71.4)	14 (93.3)	0.226
BMI, kg/m^2	21.2 ± 2.9	21.8 ± 3.4	0.582
LVEF, %	53.3 ± 10.5	23.3 ± 5.3	<0.001***
Medical History, n (%)			
Hypertension	7 (33.3)	2 (13.3)	0.329
Diabetes mellitus	1 (4.8)	2 (13.3)	0.760
CHD	1 (4.8)	2 (13.3)	0.760
Preoperative Medication, n (%)			
ACEI	7 (33.3)	2 (13.3)	0.329
BB	2 (9.5)	2 (13.3)	1.000
CCB	2 (9.5)	0 (0)	0.225

CAVD, calcific aortic valve disease; BMI, body mass index; LVEF, left ventricle ejection fraction; CHD, coronary heart disease; ACEI, angiotensin converting enzyme inhibitors; BB, beta-blockers; CCB, calcium-channel blockers.
***$p < 0.001$.

Table 2. Primer Sequence

Gene	Primer Sequence
hsa-Runx2- forward	CTGTGGTTACTGTCATGGCG
hsa-Runx2- reverse	AGGTAGCTACTTGGGGAGGA
hsa-Sp7- forward	GCCCACCTACCCATCTGACTT
hsa-Sp7- reverse	GTGCGAAGCCTTGCCATACA
hsa-OPN- forward	TCACCTGTGCCATACCAGTT
hsa-OPN- reverse	TGTGGTCATGGCTTTCGTTG
hsa-ATF4- forward	CACCGCAACATGACCGAAAT
hsa-ATF4- reverse	TACCCAACAGGGCATCCAAG
hsa-GAPDH- forward	GCTCAACGTGTGGTCATCTC
hsa-GAPDH - reverse	ACCCTTCCACGATCCCAAAT
hsa-miR-214-3p-forward	ACAGCAGGCACAGACAGGCAG

Transient Transfection

VICs were seeded at a density of 4×10^5 cells in 6-well plates. When the VICs reached 70%–80% confluence, they were individually transfected with 100 pmol miR-214 agomiR, 100 pmol miR-214 antagomiR (GenePharma, Shanghai, China), and 10 μg Sp7 siRNA or ATF4 siRNA (Obio Technology, Shanghai, China) in Opti-MEM (Invitrogen, USA) using lipofectamine 2000 (Thermo Scientific, USA), according to the manufacturer's protocol. The medium was then changed to osteogenic medium after 6–8 h.

mRNA and microRNA Quantitative Real-Time PCR

Total RNA, including microRNAs and mRNAs, were extracted by Trizol Regent Kit (RNAiso Plus, Takara, Japan) following the manufacturer's protocol. For mRNA quantification, cDNA was synthesized from 1 μg of total RNA using the PrimeScript RT reagent Kit (Takara, Japan). MicroRNAs were extracted as previously mentioned and reverse transcribed by miRNA First Strand Synthesis Kit (Clontech, Takara, Japan). TB Green real-time-PCR Kit (Takara, Japan) and LightCycler 480 System (Roche, Switzerland) were used for quantitative real-time PCR analysis. Amplification conditions were set as follows: 95°C for 3 min, 40 cycles of denaturation at 95°C for 30 s, annealing at 62°C for 30 s, and final extension at 72°C for 30 s. The mRNA and microRNA expression were normalized to the reference gene GAPDH and U6 levels for each cDNA sample, respectively. All results were compared to the expression level at baseline by $2^{-\Delta\Delta Ct}$ method. The primers used in this experiment are presented in Table 2.

Alizarin Red Staining

Alizarin red staining was performed after 7 days of osteogenic differentiation procedure. Briefly, VICs were washed twice with PBS, then fixed by 75% ethanol for 10 min at room temperature and washed with distilled water. Finally, VICs were stained by Alizarin red solution (Servicebio, Wuhan, China) at room temperature for 10 min. The VICs were washed three times with 95% ethanol to remove non-specific staining. Matrix calcification in alizarin red staining was manifested with red deposition. The stained matrix was assessed and photographed using a digital microscope. Alizarin red stain was released from the cell matrix by incubation with 10% acetic acid solution for 10 min. The absorbance was quantified by spectrophotometry at 450 nm. Paraffin sections were stained by alizarin red solution for 5 min after the consecutive procedures of sectioning, dewaxing, and hydrating.

H&E Staining and VB Staining

A slicing machine was used to cut aortic valve specimens into 5-μm-thick paraffin sections. Then, a routine protocol was conducted: sectioning, dewaxing, and hydrating. Paraffin sections were stained with hematoxylin and eosin (H&E) solution consecutively for 3 min and 1 min. The rehydrated sections were stained with Victoria Blue (VB) solution and Ponceau S Staining Kit consecutively for 1 h and 1min.

Dual Luciferase Reporter Assay

The WT ATF4 or Sp7-3′-UTR containing the predicted miR-214 binding site was cloned into the psiCHECK-2 vector (Sangon Biotech, Shanghai, China) utilizing the Xhol and Notl restriction sites. 293T cells were seeded in 24-well plates, and then 4 μg luciferase reporter plasmid and 25 pmol miR-214 agomiR or agomir-NC were co-transfected using Lipofectamine 2000 (Thermo Scientific, USA). After transfection for 48 h, firefly and Renilla luciferase activities were consecutively measured using the dual luciferase reporter assay system (Promega, USA) under the guidance of the manufacturer's protocol.

Western Blotting

After each treatment, VICs were washed with PBS and lysed in SDS buffer containing a protease inhibitor cocktail (1:100) on ice for 30 min. Total protein concentrations were evaluated using a protein

assay kit (Beyotime Biotech, Shanghai, China). Cell lysate was separated using 10% SDS-PAGE and then transferred to polyvinylidene difluoride membranes. Subsequently, the membranes were blocked for 1 h at room temperature by incubation in tris buffered saline tween (TBST) solution containing 5% (w/v) nonfat milk. Primary antibodies against Runx2 (CST, #12556, 1:500), Osterix (abcam, ab22552, 1:1,000), OPN (abcam, ab8448, 1:800), ATF4 (Santa Cruz, sc-390063, 1:50), and GAPDH (Protein tech, 60004-1-Ig, 1:5000) were incubated overnight at 4°C. Finally, the membranes were incubated with appropriate secondary antibodies (Jackson Immuno Research, 115-035-003, 1:5,000) for 1 h at room temperature and detected with an ECL kit (Thermo Scientific, USA) and then exposed to film.

Immunohistochemistry

The procedures from beginning to hydrating were identical to H&E staining. After block procedure, primary antibodies were applied at optimized concentrations and incubated overnight at 4°C. Subsequently, the positive staining was detected by UltraSensitive SP IHC Kit and DAB Kit (Maixin Biotech, Fujian, China). Nuclei counterstaining was achieved by staining with hematoxylin. The primary antibodies used in this study included Runx2 (abcam, ab23981, 1:200), OPN (abcam, ab8448, 1:200), Osterix (abcam, ab22552, 1:200), ATF4 (Affinity, DF6008, 1:100), and OCN (abcam, ab13420, 1:200).

Immunofluorescence

Briefly, VICs grown on 24-wells plates were fixed with 4% paraformaldehyde for 30 min at room temperature. Permeabilization was achieved by 0.5% Triton X-100, and VICs were then blocked for 0.5 h at room temperature using BSA (Maixin Biotech, Fujian, China). Primary antibodies against Vimentin (Santa Cruz, sc-6260, USA), α-SMA (Affinity, AF1032, USA), and CD31 (Abcam, ab28364, USA) were incubated overnight at 4°C. Subsequently, VICs were incubated with corresponding secondary antibodies labeled with fluorescein isothiocyanate (FITC; Servicebio, GB22301, Wuhan, China) for 1 h at room temperature. Nuclei were stained with 4′,6-diamidino-2-phenylindole (Servicebio, GB22301, Wuhan, China) for 5 min. Fluorescent images were acquired using an inverted fluorescent microscope.

Animal Experiments

The animal studies were approved by the ethics committee institution of Second Military Medical University; all experimental protocols complied with the NIH Guide. The gene sequence of the miR-214 knockout rat is shown in Figure S1. The genotype of rats was identified by a combination of agarose electrophoresis and quantitative real-time PCR at day 7 after birth. Then, male rats were subdivided into 3 groups (n = 6 for each group), including WT, heterozygote, and knockout. The CAVD model was constructed by Western diet for 4 months; at the same time, vitamin D_2 (Sigma, USA) was injected intraperitoneally every 2 days (25,000 IU/kg) during the first month. Transthoracic echocardiography of rats was performed at the end of the experiment under sedation by inhalation of 2% isoflurane. Ultrasound images were obtained by using a probe (M5Sc-D, GE, USA) combined with Vivid E95 (GE, USA). Parasternal short-axis view, long-axis view, and apical five-chamber view were used to measure the aortic area, mean transvalvular gradient, and velocity. All echocardiographic imaging and analyses were collected by the same experienced investigator blinded to the assignments. The rats were sacrificed, and the heart was fixed with 10% formalin after dissection for further study.

Statistical Analysis

Continuous data are expressed as the mean ± standard deviation, and categorical variables are stated as absolute numbers and proportions. Statistical analysis was performed with GraphPad and SPSS software. Normally distributed variables were analyzed using Student's t test, and non-normally distributed variables were analyzed using Mann-Whitney U test. p value <0.05 was considered statistically significant for all tests.

SUPPLEMENTAL INFORMATION

Supplemental Information can be found online at https://doi.org/10.1016/j.omtn.2020.10.016.

AUTHOR CONTRIBUTIONS

X.H.L. and Z.X. conceived this study. N.L., Y.B., and G.Z. designed and performed experiments. M.S., X.S., and X.Z. performed animal experiments, Y.M., M.T., F.Q., and X.L. analyzed data and prepared the manuscript and critically discussed the data. X.H.L. and Z.X. revised the article. All authors read and approved the final manuscript.

CONFLICT OF INTEREST

The authors declare no competing interests.

ACKNOWLEDGMENTS

This work was supported by National Natural Science Foundation of China (grant nos. 81570351, 81570208, 81600307, 81870287, and 82070419) and the National Key Research and Development Program of China (grant no. 2016YFC1100900).

REFERENCES

1. Lindman, B.R., Clavel, M.A., Mathieu, P., Iung, B., Lancellotti, P., Otto, C.M., and Pibarot, P. (2016). Calcific aortic stenosis. Nat. Rev. Dis. Primers *2*, 16006.

2. Small, A., Kiss, D., Giri, J., Anwaruddin, S., Siddiqi, H., Guerraty, M., Chirinos, J.A., Ferrari, G., and Rader, D.J. (2017). Biomarkers of Calcific Aortic Valve Disease. Arterioscler. Thromb. Vasc. Biol. *37*, 623–632.

3. Myasoedova, V.A., Ravani, A.L., Frigerio, B., Valerio, V., Moschetta, D., Songia, P., and Poggio, P. (2018). Novel pharmacological targets for calcific aortic valve disease: Prevention and treatments. Pharmacol. Res. *136*, 74–82.

4. Gould, S.T., Srigunapalan, S., Simmons, C.A., and Anseth, K.S. (2013). Hemodynamic and cellular response feedback in calcific aortic valve disease. Circ. Res. *113*, 186–197.

5. Zhao, Y., Zhou, J., Liu, D., Dong, F., Cheng, H., Wang, W., Pang, Y., Wang, Y., Mu, X., Ni, Y., et al. (2015). ATF4 plays a pivotal role in the development of functional hematopoietic stem cells in mouse fetal liver. Blood *126*, 2383–2391.
6. Greenblatt, M.B., Shim, J.H., and Glimcher, L.H. (2013). Mitogen-activated protein kinase pathways in osteoblasts. Annu. Rev. Cell Dev. Biol. *29*, 63–79.
7. Cao, H., Yu, S., Yao, Z., Galson, D.L., Jiang, Y., Zhang, X., Fan, J., Lu, B., Guan, Y., Luo, M., et al. (2010). Activating transcription factor 4 regulates osteoclast differentiation in mice. J. Clin. Invest. *120*, 2755–2766.
8. Zhang, Y., Lin, T., Lian, N., Tao, H., Li, C., Li, L., and Yang X. (2019). Hop2 Interacts with ATF4 to Promote Osteoblast Differentiation. J. Bone Miner. Res. *34*, 2287–2300.
9. Li, D., Liu, J., Guo, B., Liang, C., Dang, L., Lu, C., He, X., Cheung, H.Y., Xu, L., Lu, C., et al. (2016). Osteoclast-derived exosomal miR-214-3p inhibits osteoblastic bone formation. Nat. Commun. *7*, 10872.
10. Wang, X., Guo, B., Li, Q., Peng, J., Yang, Z., Wang, A., Li, D., Hou, Z., Lv, K., Kan, G., et al. (2013). miR-214 targets ATF4 to inhibit bone formation. Nat. Med. *19*, 93–100.
11. Lee, Y.B., Bantounas, I., Lee, D.Y., Phylactou, L., Caldwell, M.A., and Uney, J.B. (2009). Twist-1 regulates the miR-199a/214 cluster during development. Nucleic Acids Res. *37*, 123–128.
12. Zhao, C., Sun, W., Zhang, P., Ling, S., Li, Y., Zhao, D., Peng, J., Wang, A., Li, Q., Song, J., et al. (2015). miR-214 promotes osteoclastogenesis by targeting Pten/PI3k/Akt pathway. RNA Biol. *12*, 343–353.
13. Sun, Y., Kuek, V., Liu, Y., Tickner, J., Yuan, Y., Chen, L., Zeng, Z., Shao, M., He, W., and Xu, J. (2018). MiR-214 is an important regulator of the musculoskeletal metabolism and disease. J. Cell. Physiol. *234*, 231–245.
14. Watanabe, T., Sato, T., Amano, T., Kawamura, Y., Kawamura, N., Kawaguchi, H., Yamashita, N., Kurihara, H., and Nakaoka, T. (2008). Dnm3os, a non-coding RNA, is required for normal growth and skeletal development in mice. Dev. Dyn. *237*, 3738–3748.
15. Roberto, V.P., Gavaia, P., Nunes, M.J., Rodrigues, E., Cancela, M.L., and Tiago, D.M. (2018). Evidences for a New Role of miR-214 in Chondrogenesis. Sci. Rep. *8*, 3704.
16. Yang, L., Ge, D., Cao, X., Ge, Y., Chen, H., Wang, W., and Zhang, H. (2016). MiR-214 Attenuates Osteogenic Differentiation of Mesenchymal Stem Cells via Targeting FGFR1. Cell Physiol. Biochem *38*, 809–820.
17. Liu, M., Sun, Y., and Zhang, Q. (2018). Emerging Role of Extracellular Vesicles in Bone Remodeling. J. Dent. Res. *97*, 859–868.
18. Sun, W., Zhao, C., Li, Y., Wang, L., Nie, G., Peng, J., Wang, A., Zhang, P., Tian, W., Li, Q., et al. (2016). Osteoclast-derived microRNA-containing exosomes selectively inhibit osteoblast activity. Cell Discov. *2*, 16015.
19. Rathan, S., Ankeny, C.J., Arjunon, S., Ferdous, Z., Kumar, S., Fernandez Esmerats, J., Heath, J.M., Nerem, R.M., Yoganathan, A.P., and Jo, H. (2016). Identification of side- and shear-dependent microRNAs regulating porcine aortic valve pathogenesis. Sci. Rep. *6*, 25397.
20. Salim, M.T., Esmerats, J.F., Arjunon, S., Villa-Roel, N., Nerem, R.M., Jo, H., and Yoganathan, A.P. (2019). miR-214 is Stretch-Sensitive in Aortic Valve and Inhibits Aortic Valve Calcification. Ann. Biomed. Eng. *47*, 1106–1115.
21. Coffey, S., Williams, M.J., Phillips, L.V., Galvin, I.F., Bunton, R.W., and Jones, G.T. (2016). Integrated microRNA and messenger RNA analysis in aortic stenosis. Sci. Rep. *6*, 36904.
22. Song, R., Fullerton, D.A., Ao, L., Zhao, K.S., Reece, T.B., Cleveland, J.C., Jr., and Meng, X. (2017). Altered MicroRNA Expression Is Responsible for the Pro-Osteogenic Phenotype of Interstitial Cells in Calcified Human Aortic Valves. J. Am. Heart Assoc. *6*, e005364.
23. Wang, H., Shi, J., Li, B., Zhou, Q., Kong, X., and Bei, Y. (2017). MicroRNA Expression Signature in Human Calcific Aortic Valve Disease. BioMed Res. Int. *2017*, 4820275.
24. Zheng, D., Zang, Y., Xu, H., Wang, Y., Cao, X., Wang, T., Pan, M., Shi, J., and Li, X. (2019). MicroRNA-214 promotes the calcification of human aortic valve interstitial cells through the acceleration of inflammatory reactions with activated MyD88/NF-κB signaling. Clin. Res. Cardiol. *108*, 691–702.
25. Gupta, S.K., Kumari, S., Singh, S., Barthwal, M.K., Singh, S.K., and Thum, T. (2020). Non-coding RNAs: Regulators of valvular calcification. J. Mol. Cell. Cardiol. *142*, 14–23.
26. Masuda, M., Miyazaki-Anzai, S., Levi, M., Ting, T.C., and Miyazaki, M. (2013). PERK-eIF2α-ATF4-CHOP signaling contributes to TNFα-induced vascular calcification. J. Am. Heart Assoc. *2*, e000238.
27. Fu, Z., Li, F., Jia, L., Su, S., Wang, Y., Cai, Z., and Xiang, M. (2019). Histone deacetylase 6 reduction promotes aortic valve calcification via an endoplasmic reticulum stress-mediated osteogenic pathway. J. Thorac. Cardiovasc. Surg. *158*, 408–417.e2.
28. Cai, Z., Li, F., Gong, W., Liu, W., Duan, Q., Chen, C., Ni, L., Xia, Y., Cianflone, K., Dong, N., and Wang, D.W. (2013). Endoplasmic reticulum stress participates in aortic valve calcification in hypercholesterolemic animals. Arterioscler. Thromb. Vasc. Biol. *33*, 2345–2354.
29. Wang, W., Lian, N., Ma, Y., Li, L., Gallant, R.C., Elefteriou, F., and Yang, X. (2012). Chondrocytic Atf4 regulates osteoblast differentiation and function via Ihh. Development *139*, 601–611.
30. Ducy, P., and Karsenty, G. (1995). Two distinct osteoblast-specific cis-acting elements control expression of a mouse osteocalcin gene. Mol. Cell. Biol. *15*, 1858–1869.
31. Elefteriou, F., Benson, M.D., Sowa, H., Starbuck, M., Liu, X., Ron, D., Parada, L.F., and Karsenty, G. (2006). ATF4 mediation of NF1 functions in osteoblast reveals a nutritional basis for congenital skeletal dysplasiae. Cell Metab. *4*, 441–451.
32. Zhuo, Z., Wan, Y., Guan, D., Ni, S., Wang, L., Zhang, Z., Liu, J., Liang, C., Yu, Y., Lu, A., et al. (2020). A Loop-Based and AGO-Incorporated Virtual Screening Model Targeting AGO-Mediated miRNA-mRNA Interactions for Drug Discovery to Rescue Bone Phenotype in Genetically Modified Mice. Adv. Sci. (Weinh.) *7*, 1903451.
33. Wang, C., Sun, W., Ling, S., Wang, Y., Wang, X., Meng, H., Li, Y., Yuan, X., Li, J., Liu, R., et al. (2019). AAV-Anti-miR-214 Prevents Collapse of the Femoral Head in Osteonecrosis by Regulating Osteoblast and Osteoclast Activities. Mol. Ther. Nucleic Acids *18*, 841–850.
34. Li, K.C., Chang, Y.H., Yeh, C.L., and Hu, Y.C. (2016). Healing of osteoporotic bone defects by baculovirus-engineered bone marrow-derived MSCs expressing MicroRNA sponges. Biomaterials *74*, 155–166.
35. Sun, Y., Ye, X., Cai, M., Liu, X., Xiao, J., Zhang, C., Wang, Y., Yang, L., Liu, J., Li, S., et al. (2016). Osteoblast-Targeting-Peptide Modified Nanoparticle for siRNA/microRNA Delivery. ACS Nano *10*, 5759–5768.